1980-07

Finite-amplitude standing waves within real cavities

Coppens, Alan B.; Sanders, James V.

Acoustical Society of America

Coppens, Alan B., and James V. Sanders. "Finiteamplitude standing waves within real cavities." The Journal of the Acoustical Society of America 58.6 (1975): 1133-1140. http://hdl.handle.net/10945/63144

Finite-amplitude standing waves within real cavities

Alan B. Coppens and James V. Sanders

Naval Postgraduate School, Monterey, California 93940
(Received 9 August 1974; revised 9 June 1975)

A three-dimensional mathematical model for acoustical standing waves in lossy fluid-filled cavities has been obtained which requires empirical values for the resonance frequencies f_n and quality factors Q_n (all measured in the linear acoustic régime) of the pertinent standing waves which the cavity can support. The nonlinear distortion of the observed pressure waveform depends strongly on the f's and Q's of those standing waves excited by harmonics of the driving frequency. The model is applicable to non-ideal cavities if the deviations from idealized geometry and boundary conditions are small. It is restricted to small values of $M(1+1/2\ B/A)Q_1$, where M is the peak Mach number and Q_1 the quality factor of the fundamental component of the driven standing wave, and B/A is the parameter of nonlinearity of the fluid. Comparisons between the model and experiment are made for a rectangular cavity driven in one- and two-dimensional modes. Agreement is excellent except when there are degeneracies involving the predicted nonlinearly excited standing waves and other standing waves of the cavity. Small discrepancies appear to result from the coupling of energy from the nonlinearly excited standing wave into its degenerate neighbor.

Subject Classification: 25.25; 55.20.

LIST OF SYMBOLS

B/A ratio of coefficients in the approximate isentropic equation of state $p=(A/\rho_0)(\rho-\rho_0)+[B/(2\rho_0^2)]\times(\rho-\rho_0)^2$
$c^2\Box^2$ $=c^2\nabla^2-\partial^2/\partial t^2$
c_0^2 $=(dP/d\rho)$ at $\rho=\rho_0$
c_n effective phase speed associated with a standing wave at resonance (Eqs. 9 and 12)
C_p specific heat at constant pressure
k propagation constant associated with a standing wave (Eq. 6)
K thermal conductivity
M peak Mach number of the driven standing wave
p $=P-P_0\doteq-\rho_0\,\partial\Phi/\partial t=$ acoustic pressure
P, P_0 instantaneous and equilibrium total pressure in the field
$\mathcal{P}$ Prandtl number $=\eta C_p/K$
Q_n quality factor of a resonance $\doteq\omega_n/(2\alpha_n c_0)$
$\mathbf{u}$ particle velocity
$\alpha_n c_0$ temporal decay constant of a resonance
β $=(\gamma+1)/2$ for a gas or $1+\frac{1}{2}B/A$ for a liquid
γ ratio of specific heats for a gas or $1+B/A$ for a liquid
η shear viscosity
ρ, ρ_0 instantaneous and equilibrium densities of the fluid
Φ velocity potential
ω (angular) frequency at which the cavity is driven
ω_n (angular) frequency of a resonance

INTRODUCTION

This paper* describes the extension of an investigation of finite-amplitude standing waves reported previously.[1] In this earlier work, dealing with relatively small values of a strength parameter $M\beta Q_1$, solutions of the nonlinear wave equation with *theoretically* predicted absorption coefficients and phase speeds were consistent with the observed finite-amplitude distortion. Later experimental investigations[2] disclosed small but significant differences: While the absorption coefficients were nearly as predicted by the classical theory[3] for wall losses, the resonance frequencies of the tube deviated slightly from predictions. This suggested that unaccounted-for realities in the tube affected the validity of the assumed model for absorption and dispersion. A modified equation with phase speeds based on the observed resonance frequencies was shown to be in better agreement with experiment.[4] As a consequence, it was decided to develop a mathematical model which would utilize the *experimentally observed* absorptive and dispersive properties of the cavity as measured in the linear régime.

I. THE NONLINEAR WAVE EQUATION

A. General

It is well known[5] that for $\alpha/k\ll1$ and $M\ll1$ loss terms and nonlinear terms in the constitutive equations can be separately approximated with the help of linear, lossless acoustic relations. If we write the force equation in the form

$$\frac{\partial\mathbf{u}}{\partial t}+(\mathbf{u}\cdot\nabla)\mathbf{u}+\frac{1}{\rho}\nabla P=\frac{1}{\rho}\mathfrak{L}\mathbf{u}, \tag{1}$$

where the operator $\mathfrak{L}$ describes those physical processes leading to absorption and dispersion, ignore rotational effects so that

$$\mathbf{u}=\nabla\Phi, \tag{2}$$

restrict attention to plane waves or standing waves in rectangular cavities, and neglect terms of orders higher than M^2, $M(\alpha/k)$, and $(\alpha/k)^2$, the result is a quadratically nonlinear wave equation,

$$\left(c_0^2\Box^2+\frac{\partial}{\partial t}\mathfrak{L}\right)\frac{p}{\rho_0c_0^2}\doteq-\frac{\partial^2}{\partial t^2}\left[\left(\frac{u}{c_0}\right)^2+\frac{\gamma-1}{2}\left(\frac{p}{\rho_0c_0^2}\right)^2\right]. \tag{3}$$

[For plane-wave propagation in a circular duct of radius R the dominant loss term can arise from the shear and thermal waves generated at the boundary, and we have[1,3]

$$\frac{\partial}{\partial t}\mathfrak{L}=\frac{1}{R}\left(\frac{2\eta}{\omega\rho_0}\right)^{1/2}\left(1+\frac{\gamma-1}{\sigma^{1/2}}\right)\left(\frac{1}{\omega}\frac{\partial^3}{\partial x^2\partial t}-\frac{\partial^2}{\partial x^2}\right), \tag{4}$$

so that $\mathfrak{L}$ contributes both absorptive and dispersive terms.]

The left-hand side of Eq. 3 is the classical, linear wave equation pertinent to the system under study. The right-hand side can be interpreted as a forcing function consisting of a three-dimensional spatial distribution of phase-coherent sources. In a second-order perturbation theory, this forcing function is obtained from the classical (first-order) solution of the acoustical problem. The second-order perturbation solution describes the nonlinearities resulting from the self interaction of the classical solution. Higher-order perturbation solutions consider the interaction of the nonlinear solution with itself, and the forcing function is composed of products of both classical and nonlinearly generated terms. Thus, if a system is driven at frequency ω, the nonlinear term in Eq. 3 will force the existence of all integer multiples $n\omega$ of the driving frequency and the full solution must contain all harmonics of the input frequency. In a closed cavity, each of those nonlinearly generated waves whose frequency lies close to the resonance frequency of a standing wave of the cavity and whose associated spatial function matches that of the standing wave can be strongly excited. Just how strongly will depend on the quality factor Q for the particular resonance and the difference between the resonance frequency of the standing wave and the harmonic $n\omega$.

B. The rectangular cavity

1. Formulation

If a rigid cavity of dimensions L_x, L_y, L_z is driven acoustically at frequency ω, the resultant pressure standing wave is of the form

$$\cos k_x x\cos k_y y\cos k_z z\cos\omega t, \tag{5}$$

where the k's satisfy the conditions

$$k_xL_x=m_x\pi,\quad k_yL_y=m_y\pi,\quad k_zL_z=m_z\pi, \tag{6}$$

and the m's are integers. The right-hand side of Eq. 3 will contain terms of the form

$$(n\omega)^2D\cos n_xk_xx\cos n_yk_yy\cos n_zk_zz\cos(n\omega t+\varphi), \tag{7}$$

where n, n_x, n_y, and n_z are integers and φ and D depend on the particular values of the n's. The response of the cavity to each of these forcing functions depends upon how closely Eq. 7 corresponds to a standing wave of the cavity. A suitable trial solution appropriate to the forcing function given by Eq. 7 is

$$p/(\rho_0c_0^2)=G_nD\cos n_xk_xx\cos n_yk_yy\cos n_zk_zz\sin(n\omega t+\varphi-\theta_n). \tag{8}$$

Substitution of Eqs. 7 and 8 into Eq. 3 results in the determinations of G_n and θ_n.

The standing waves which can be excited in any real cavity deviate from the predictions of the linear wave equation with ideal boundary conditions for the following reasons: (a) The presence of boundary-layer losses at the cavity surfaces yields a dispersive contribution to the wave equation (analogous to that in Eq. 4). (b) Geometrical irregularities alter the effective dimensions of the cavity. We can treat both of these mechanisms as equivalent as long as the shifts in frequency are so small that the actual resonances are close to the theoretical values resulting from the classical model. Define the resonance frequencies for each of the standing waves,

$$\omega_n=c_n[(n_xk_x)^2+(n_yk_y)^2+(n_zk_z)^2]^{1/2}, \tag{9}$$

where c_n is the phase speed appropriate for that frequency, and consider two limiting cases.

(1) If the forcing function does not have its frequency $n\omega$ close to ω_n, this standing wave is being forced at a frequency far removed from its resonance. Since this yields the inequality

$$\left|c_0^2\Box^2p\right|\gg\left|\frac{\partial}{\partial t}\mathfrak{L}p\right|, \tag{10}$$

losses can be ignored in Eq. 3. The value of G_n for the resulting standing wave is

$$G_n=(n\omega)^2/\left|(n\omega)^2-\omega_n^2\right|, \tag{11}$$

and the phase angle θ_n is very nearly $\pi/2$ in magnitude.

(2) If $n\omega\sim\omega_n$, then the standing wave is being forced near resonance, and losses must be retained in Eq. 3. The value of c_n can be determined from the apparent dimensions of the cavity and the measured resonance frequency ω_n. The losses are described by the measured Q_n of the resonance. This means that the linear wave-equation operator for the system can be written as

$$c_0^2\Box^2+\frac{\partial}{\partial t}\mathfrak{L}\doteq c_n^2\Box^2-\frac{n\omega}{Q_n}\frac{\partial}{\partial t}, \tag{12}$$

and used as the right-hand side of Eq. 3. The phase angle θ_n is now given by

$$\tan\theta_n=-F_n, \tag{13}$$

where the frequency parameter F_n is defined as

$$F_n=Q_n[(n\omega)^2-\omega_n^2]/(n\omega)^2. \tag{14}$$

For $\Delta\omega_n/\omega_n\ll1$, where

$$\Delta\omega_n=n\omega-\omega_n, \tag{15}$$

Eq. 14 becomes

$$F_n\doteq2Q_n(\Delta\omega_n/\omega_n). \tag{16}$$

The amplitude factor G_n is

$$G_n=Q_n\cos\theta_n. \tag{17}$$

Thus, the resonance parameters Q_n and ω_n of the standing wave are important in determining its amplitude and phase in response to the forcing function.

Comparison of cases (1) and (2) reveals that the re-

sponse of the cavity when $n\omega \neq \omega_n$ is of order $1/Q$ compared to that when $n\omega \sim \omega_n$. Thus, for the high-Q resonances usually encountered in cavities with rigid walls, we can ignore those components in the forcing function which excite standing waves far from resonance compared to those components exciting standing waves near resonance.

In a rectangular cavity, the standing waves fall into *families* (nm_x, nm_y, nm_z), where n and the m's are integers. The inequality between each of the resonance frequencies ω_n of the members of the family and the appropriate harmonic $n\omega_1$ of the first (lowest) member is measured by

$$e_n = (\omega_n - n\omega_1)/n\omega_1 . \tag{18}$$

2. Solution near resonance

The previous discussion has shown that "nonresonant" terms can be neglected with respect to the "nearly resonant" terms if a rectangular cavity is being driven near a resonance. We can therefore simplify Eq. 3 by writing the total standing wave as

$$p = \sum_{n=1}^{\infty} p_n , \tag{19a}$$

where each p_n is of frequency $n\omega$ and has the form

$$p_n/(\rho_0 c_0^2) = MR_n \cos nk_x x \cos nk_y y \cos nk_z z \sin(n\omega t + \phi_n). \tag{19b}$$

These p_n's constitute the family of normal modes nearly resonant with the harmonics of the frequency exciting p_1. Since M has been specified as the peak Mach number of the fundamental standing wave p_1, the coefficient R_1 must be unity. Further, since time can be referenced to any convenient instant, we choose $\phi_1 = 0$ so that the fundamental of the pressure wave behaves like $\cos\omega t$.

Combination of Eqs. 3, 12, and 19a yields

$$\sum_n \left(c_n^2 \Box^2 - \frac{n\omega}{Q_n}\frac{\partial}{\partial t}\right)\frac{p_n}{\rho_0 c_0^2} \doteq -\frac{\partial^2}{\partial t^2}\left[\left(\frac{u}{c_0}\right)^2 + \frac{\gamma-1}{2}\left(\frac{p}{\rho_0 c_0^2}\right)^2\right], \tag{20a}$$

where u must be obtained from

$$u \doteq -\nabla \int (p/\rho_0)\, dt . \tag{20b}$$

Nonresonant contributions on the right-hand side of Eq. 20a lead to negligibly small nonresonant solutions which have already been neglected in Eq. 19. If p and u are squared in the right-hand side of Eq. 20 and all powers of sines and cosines reduced to series of sines and cosines, we can ignore all terms except those which constitute the family built on p_1. For more details, refer to the Appendix.

Substituting Eq. 19 into Eq. 20, retaining just nearly resonant terms, and then equating like terms in space and time results in a set of coupled, nonlinear, transcendental equations, each of the form

$$R_n \begin{Bmatrix}\cos\\ \sin\end{Bmatrix}(\phi_n - \theta_n) = NM\beta Q_n \cos\theta_n \left(\frac{1}{2}\sum_{j=1}^{n-1} R_j R_{n-j} \begin{Bmatrix}\cos\\ \sin\end{Bmatrix}(\phi_j + \phi_{n-j}) - \sum_{j=1}^{\infty} R_{n+j}R_j \begin{Bmatrix}\cos\\ \sin\end{Bmatrix}(\phi_{n+j} - \phi_j)\right) \tag{21}$$

for all $n > 1$. The values of Q_n and ω_n must be determined from the infinitesimal-amplitude behavior of the cavity. The Mach number M and driving frequency ω are known. The phase angles θ_n are given by Eqs. 13 and 16, and N has the value

$$\begin{aligned} N &= \tfrac{1}{2} \text{ for a one-dimensional standing wave,}\\ &= \tfrac{1}{4} \text{ for a two-dimensional standing wave,}\\ &= \tfrac{1}{8} \text{ for a three-dimensional standing wave.} \end{aligned} \tag{22}$$

For the same value of strength parameter, the nonlinear term is weakened appreciably for two- and three-dimensional waves by the decreasing value of N.

Equation 21 can be solved by a method of successive approximations on a digital computer. This has been done for comparison with the experimental results discussed in the second half of this paper.

3. Approximate lower-order solution and consonance

If the $M\beta Q_n$'s are sufficiently small, then only the leading terms of the lowest harmonics need be retained and a solution can be found without having to use successive approximations. Simple expressions result which serve to illustrate the effects of the properties of the cavity on the finite-amplitude distortion process.

For small strength parameter, the R_n's decrease in value rapidly as n increases and R_2 and ϕ_2 are determined by the interaction of the fundamental with itself,

$$R_2 \doteq \tfrac{1}{2} NM\beta Q_2 \cos\theta_2 \tag{23}$$

and

$$\phi_2 \doteq \theta_2 = -\arctan F_2 . \tag{24}$$

For small $M\beta Q_2$ the second harmonic depends only on M, Q_2, and F_2. Notice that R_2 is maximized at a frequency $\omega = \omega_2/2$ for constant M.

The interaction of the second harmonic with the fundamental yields

$$R_3 \doteq \tfrac{1}{2} N^2 (M\beta Q_2 \cos\theta_2)(M\beta Q_3 \cos\theta_3) \tag{25}$$

and

$$\phi_3 \doteq \theta_2 + \theta_3 . \tag{26}$$

The response of the third harmonic depends on M, Q_2, F_2, Q_3, and F_3. For constant M the greatest *driving* of the third member occurs at $\omega = \omega_2/2$, which maximizes the second harmonic; the greatest *response* of the standing wave to the driving function occurs when the third harmonic of the fundamental coincides with ω_3. Equation 25 reveals that when ω_2 and ω_3 are sufficiently nonconsonant, finite-amplitude distortion above the second harmonic can be appreciably reduced.

Thus, the finite-amplitude distortion of a standing wave in a cavity is strongly influenced by the relationship between the *resonance frequencies of the family of standing waves* and the *harmonics of the resonance fre-*

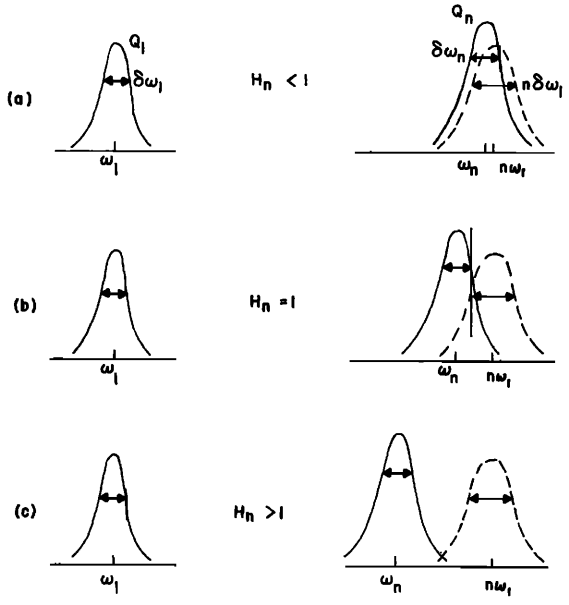

FIG. 1. The relationship between the response curve of the nth member of a family of standing waves and that of the lowest member: (a) a well-tuned situation, for which the nth member is very close to having a resonance frequency ω_n almost exactly n times that of the lowest member, (b) a less-well-tuned situation, and (c) a poorly tuned situation.

quency of its first member. To quantify this relationship, compare the resonance frequency ω_n and the quality factor Q_n of the nth member of the family with the *scaled* resonance frequency $n\omega_1$ and the quality factor Q_1 of the lowest member, as shown in Fig. 1. (The dashed response curve is that of the lowest member, transferred up to a frequency $n\omega_1$.) For $|e_n| \ll 1$, overlap of the two curves is described by a coefficient

$$H_n \doteq 2\,|e_n|\,Q_1 Q_n/(Q_1+Q_n)\,. \tag{27}$$

For values of $H_n < 1$, the response curve of the nth member overlaps considerably the dashed curve representing the lowest member, and that member can be strongly excited if all lower members also have H's less than unity. Thus, when the bandwidths of the response curves of the members of the family overlap the appropriate integer multiples of the frequencies in the bandwidth of the response curve of the lowest member, then the family is well tuned and the waveform will exhibit relatively strong nonlinear distortion. If on the other hand, there is little overlap, then the family is poorly tuned and the nonlinear distortion should be relatively weak.

II. EXPERIMENT

A. Apparatus and procedures

The apparatus employed in this experiment is identical with that previously used[1] except for two modifications. (1) The oscillator was replaced[2] by a General Radio 1161-A Coherent Frequency Synthesizer. (2) The standing-wave tube was replaced[4,6] by a rectangular cavity 30.3 by 21.0 by 7.0 cm (Fig. 2). Pressure levels within the cavity were typically around 136 dB *re* 0.0002 μbar.

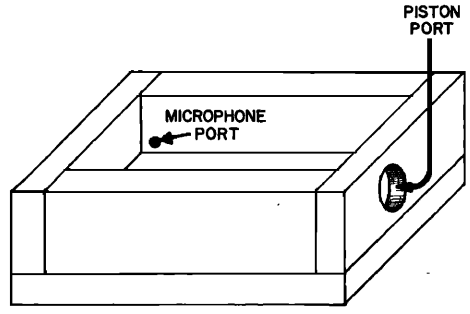

FIG. 2. View of the cavity with its top removed to show the piston and microphone ports.

The most ideal geometry exists when the face of the acoustical driver, a piston, is flush with the inside surface of the cavity. In this configuration, the observed resonance frequencies are close to those predicted by the classical, lossless theory for a perfect rectangular cavity and the resonance frequencies of a given family of standing waves are well-tuned. As the piston is moved away from this position, the shape of the cavity is perturbed and the resonance frequencies of a given family become nonharmonic.

The resonance frequencies and quality factors were determined for lower members of the family whose fundamental was to be driven and for all other standing waves whose resonance frequencies were near those of interest. For several cases, the response curve of a nonfamilial standing wave overlapped that of a family member. When this occurred, the frequencies corresponding to the observed −3, −2, and −1 dB points of the composite response curve were used to extrapolate to the resonance frequency and Q of the family member.

B. Cavity parameters

The parameters presented in Table I are typical for a well-tuned cavity. The resonance frequencies for each family closely match the harmonics of the correspond-

TABLE I. Cavity parameters for several families in the well-tuned rectangular cavity.

Mode	n	f_n	$e_n \times 10^3$	Q_n	H_n
100	1	681.00		328	
200	2	1362.39	+0.29	480	0.113
300	3	2045.02	+0.99	646	0.431
400	4	2724.11	+0.04	675	0.018
500	5	3405.95	+0.28	689	0.124
600	6	4086.57[a]	+0.14	620	0.060
010	1	817.00		379	
020	2	1633.41	−0.36	517	0.157
030	3	2449.95	−0.43	606	0.201
040	4	3266.53	−0.45	655	0.216
050	5	4081.08[a]	−0.96	772	0.488
110	1	1063.00		340	
220	2	2126.64	+0.30	447	0.116
330	3	3191.65[a]	+0.83	543	0.347
210	1	1587.00		394	
420	2	3172.51[a]	−0.47	480	0.203

[a]Near-degeneracies.

TABLE II. Cavity parameters for the $(n, n, 0)$ family for various degrees of mistunings.

Position of piston	H_2	H_3
Flush	0.115	0.347
↓	0.595	0.560
	2.12	3.23
Furthest out	3.00	7.70

ing fundamental. We can expect strong nonlinear distortion of a standing wave. Table II shows the variation in parameters for the $(n, n, 0)$ family as the piston is moved within its port. For large H_n's one would expect that the nonlinear distortion would be relatively weak.

From Table I it can be seen that the (6, 0, 0) and (0, 5, 0) standing wave are nearly degenerate, as are the (3, 3, 0) and (4, 2, 0) standing waves. The effect of these overlapping responses on the nonlinear standing wave was studied by detuning the cavity. As a measure of the amount of overlap between the nth and mth standing waves of different families, the definition in Eq. 27 was generalized with the help of Eq. 18 to

$$H_{nm} = 2\left|\frac{Q_n Q_m}{Q_n + Q_m}\frac{f_m - f_n}{f_n}\right|. \tag{28}$$

Table III illustrates the effect of detuning the cavity on the amount of overlap between nearly-degenerate pairs of standing waves.

III. RESULTS

A. The well-tuned cavity

Figures 3 and 4 illustrate the finite-amplitude behavior of the well-tuned cavity when driven at frequencies near the resonance of the (1, 0, 0) or (0, 1, 0) standing wave. The predictions of the finite-amplitude model based on the experimentally determined parameters are indicated by the solid lines. All measured harmonics peak for values of the frequency parameter lying between ±1 reflecting the fact that the resonance frequency for each family member closely matches a harmonic of the driving frequency. Agreement between experiment and theory for all one-dimensional cases studied is excellent.

The near-degeneracy noted for the (6, 0, 0) and (0, 5, 0) standing waves provides an opportunity to demonstrate

TABLE III. Effects of detuning on the amount of overlap between two typical pairs of degenerate standing waves.

Piston position	f_{600}	Q_{600}	f_{050}	Q_{050}	H_{65}
Flush	4130.23	690	4120.91	543	1.36
↓	4128.80	610	4118.62	758	1.66
Furthest out	4124.70	620	4113.67	772	1.84
Piston position	f_{330}	Q_{330}	f_{420}	Q_{420}	H_{32}
Flush	3215.02	527	3195.87	439	2.85
↓	3202.53	543	3191.22	341	1.49
Furthest out	3213.56	550	3191.93	518	3.56

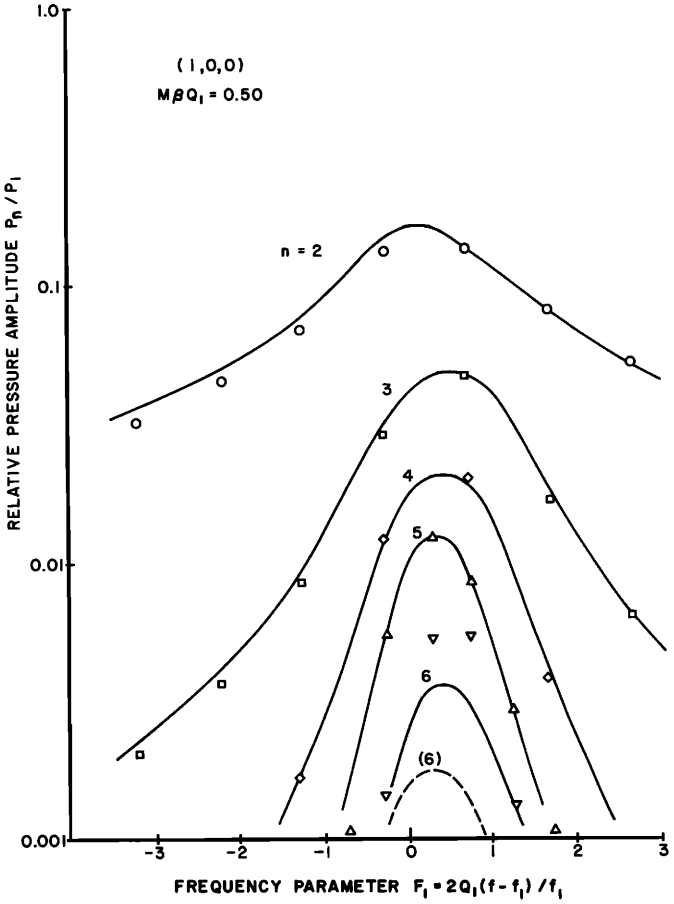

FIG. 3. Finite-amplitude distortion for excitation of the (1, 0, 0) standing wave at a strength parameter of 0.50. Cavity parameters: $Q_1 = 330$, $Q_2 = 466$, $Q_3 = 537$, $Q_4 = 587$, $Q_5 = 676$, $Q_6 = 473$; $e_2 = 0.382 \times 10^{-3}$, $e_3 = 1.065 \times 10^{-3}$, $e_4 = 0.580 \times 10^{-3}$, $e_5 = 0.470 \times 10^{-3}$, $e_6 = 1.682 \times 10^{-3}$.

the sensitivity of the model to the values of the parameters used to describe the cavity. Since the apparatus did not allow for the determination of the spatial distribution of the acoustic pressure, there was no way from the *infinitesimal-amplitude* measurements alone to sort out nearly degenerate standing waves. However, unequivocal identification is possible from the *finite-amplitude* measurements. Consider the (6, 0, 0) and (0, 5, 0) standing waves. The Q and e of each can be determined and the theoretical predictions of the harmonic distortion calculated assuming that one standing wave is the (6, 0, 0) and the other is the (0, 5, 0), and ignoring the nonfamilial standing wave. These predictions can then be recalculated by exchanging the identification of the (6, 0, 0) and (0, 5, 0) standing waves. Whichever assignment results in consistency between experiment and the model should be the correct choice. One identification results in the solid line in Fig. 3 and the other results in the dashed line. The first identification is clearly more acceptable. This same identification yields the best agreement between experiment and theory for the $(0, n, 0)$ family (Fig. 4).

B. The poorly tuned cavity

The success achieved in extending the model to two-dimensional standing waves and to poorly tuned cavities

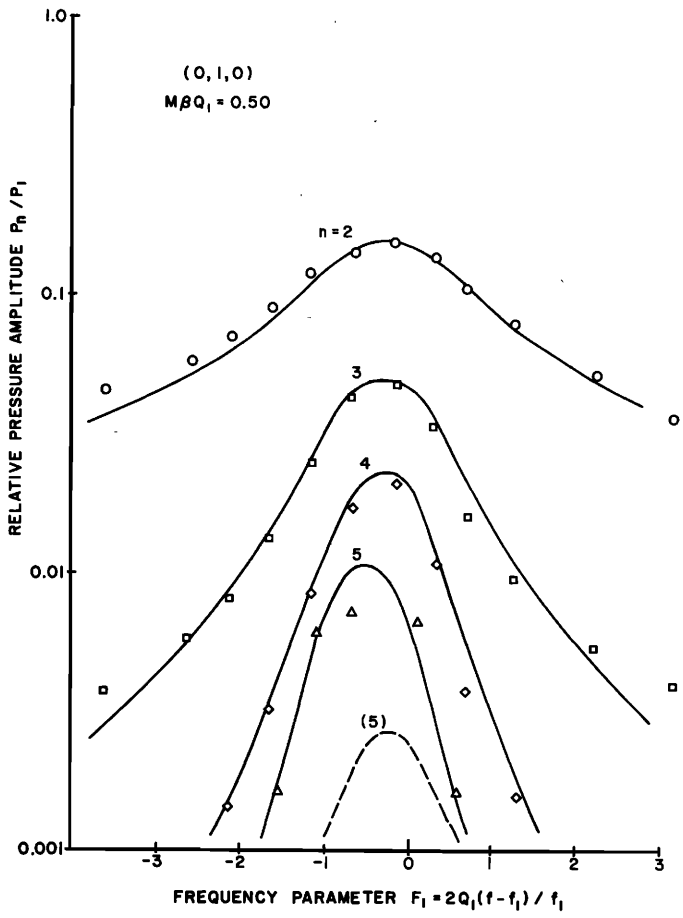

FIG. 4. Finite-amplitude distortion for excitation of the (0, 1, 0) standing wave at a strength parameter of 0.50. Cavity parameters: $Q_1=376$, $Q_2=517$, $Q_3=586$, $Q_4=662$, $Q_5=739$; $e_2=-0.384\times10^{-3}$, $e_3=-0.484\times10^{-3}$, $e_4=-0.587\times10^{-3}$, $e_5=-1.261\times10^{-3}$.

is demonstrated by the data for the (1, 1, 0) standing wave shown in Figs. 5–7. The data are displayed in order of increasing withdrawal of the piston. Even though the peak of the second-harmonic distortion occurs at frequency parameters ranging from -1 to $+3$, the results for the second harmonic are excellent. In addition, the magnitude, position, and general shape of the third-harmonic distortion are well predicted by the theory. A small systematic difference in the details of the behavior of the third harmonic centers about the frequency for which the nearly degenerate (4, 2, 0) standing wave is resonant. (This resonance lies off the graph to the left in Fig. 5 and is marked by arrows in Figs. 6 and 7.)

Support for the identification of the nearly degenerate (3, 3, 0) and (4, 2, 0) standing waves is given by the data of Fig. 8 which display the harmonic distortion obtained when the cavity was driven in the vicinity of the (2, 1, 0) standing wave. (The cavity configuration here was the same as for Fig. 7.) Besides illustrating the ability of the finite-amplitude model to identify nearly degenerate standing waves, these data show the effect of the (3, 3, 0) standing wave (whose resonance is marked with the arrow) on the second harmonic obtained when the cavity is driven near the resonance of the (2, 1, 0) standing wave.

IV. CONCLUSIONS

A one-dimensional mathematical model for finite-amplitude standing waves in a cavity has been extended to three-dimensions. Losses and dispersion, inadequately described by the classical theory of wall losses, are obtained for the *real* cavity from measurements in the *linear* acoustic régime. It has been shown that irregularities in the boundaries of the *real* cavity can be treated with an effective phase-speed dispersion—the perturbed standing wave is well represented by the unperturbed standing wave with a relatively small shift in the resonance frequency.

This model predicts that when the cavity is driven near the resonance of a standing wave the nonlinear distortion involves primarily only the family associated with the driven standing wave. The attainment of a specified amount of distortion in waves of higher dimensionality requires increased Mach number in the driving wave in the ratio of 1 : 2 : 4 for one-, two-, and three-dimensional standing waves, respectively. In all cases studied where the members of the family associated with the driven standing wave are not associated with the near degeneracies, theory and experiment are in excellent agreement.

This agreement holds for both one- and two-dimen-

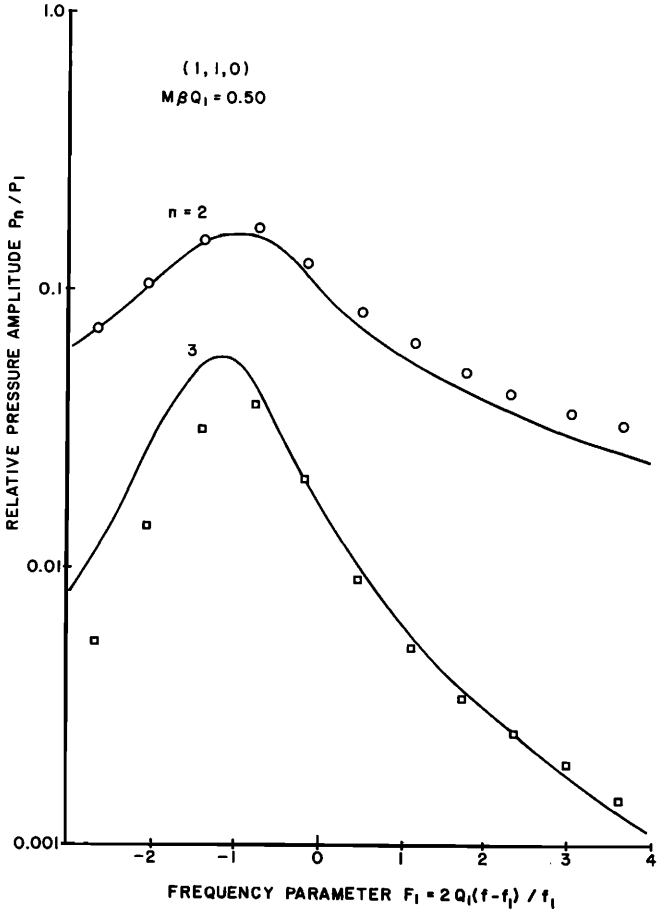

FIG. 5. Finite-amplitude distortion for excitation of the (1, 1, 0) standing wave at a strength parameter of 0.50. Cavity parameters: $Q_1=345$, $Q_2=464$, $Q_3=580$; $e_2=-1.52\times10^{-3}$, $e_3=-1.73\times10^{-3}$.

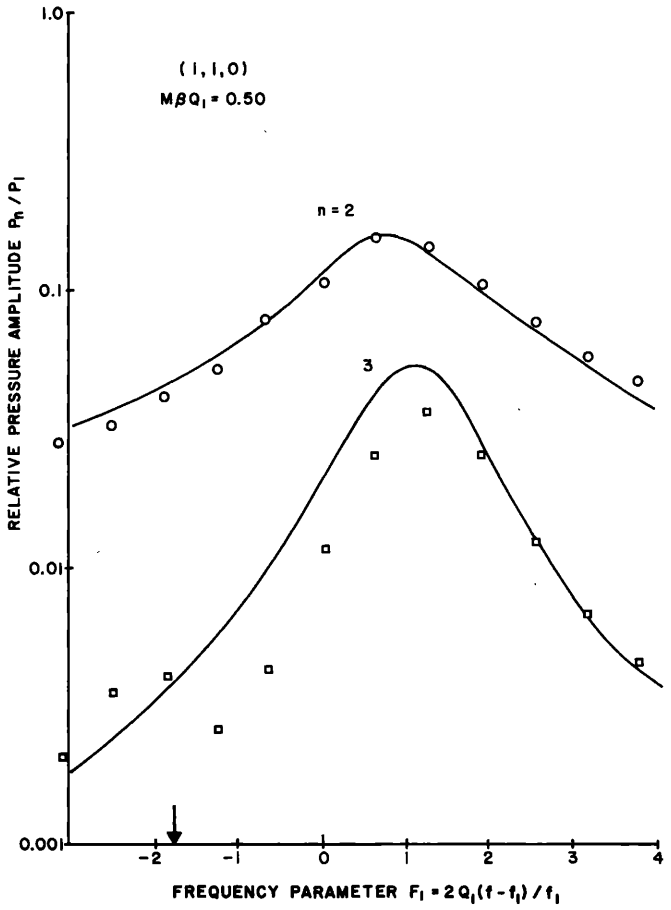

FIG. 6. Finite-amplitude distortion for excitation of the (1, 1, 0) standing wave at a strength parameter of 0.50. Cavity parameters: $Q_1 = 340$, $Q_2 = 470$, $Q_3 = 576$; $e_2 = 1.24 \times 10^{-3}$, $e_3 = 1.90 \times 10^{-3}$.

sional standing waves. While it was not possible to study three-dimensional standing waves (because of the experimental inability to determine the parameters of the closely packed standing waves involved in such cases), the agreement in two dimensions suggests that the generalization to three dimensions is valid.

When a member of the family was associated with a near degeneracy, theory and experiment still agreed well enough to differentiate unambiguously which of the nearly degenerate standing waves is a member of the family being nonlinearly excited. (Indeed, the finite-amplitude behavior of the cavity can be used to determine the identities of a pair of nearly degenerate standing waves.) However, agreement between theory and experiment is not as good as for the uncomplicated case. The results suggest a weak coupling of energy from the nonlinearly excited family into a nonfamilial standing wave which is nearly degenerate with a member of the family. This effect is not predicted by the approximate solution given by Eq. 19. Attempts to find a nonlinear excitation of these nonfamilial standing waves by retaining nonresonant terms in the solution failed. Thus, this model does not appear to provide any mechanism for the discrepancy. Detailed analysis of the experimental results at hand do not resolve whether the excitation of the nonfamilial member arises from a linear or nonlinear effect. Since this discrepancy between theory and experiment is observed to be small, the model still appears to be an adequate description of the nonlinear standing wave when there are degeneracies.

The sensitivity of the finite-amplitude theory to the parameters of the cavity suggests a method for determining the resonance frequencies and absorption properties of the cavity without resort to time-consuming infinitesimal-amplitude measurements. Comparing the measured finite-amplitude distortion to the predictions of the model would allow the determination of the appropriate parameters to describe the cavity.

ACKNOWLEDGMENTS

The theoretical work reported on in this paper was in part supported by the Office of Naval Research. The computer calculations were performed on the IBM 360 of the Randolph Church Computer Center, Naval Postgraduate School. The authors would especially like to thank Lt. Roger DeVall[6] for obtaining the data displayed in Figs. 3, 4, and 8.

APPENDIX A

We will sketch out in somewhat more detail the argument leading to the approximate form of the nonlinear solution given by Eq. 19. For ease of discussion, we

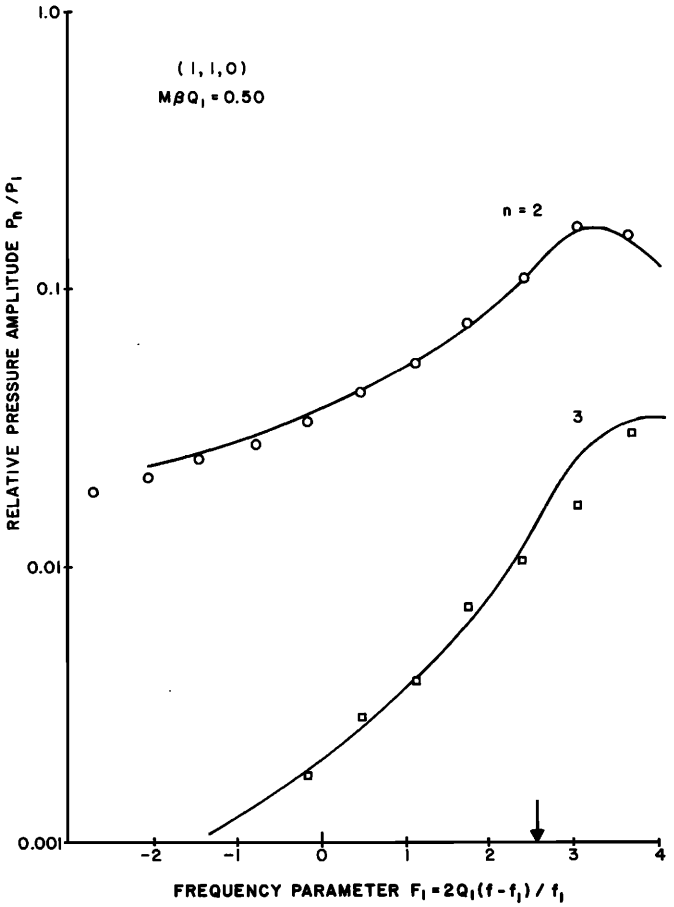

FIG. 7. Finite-amplitude distortion for excitation of the (1, 1, 0) standing wave at a strength parameter of 0.50. Cavity parameters: $Q_1 = 346$, $Q_2 = 473$, $Q_3 = 514$; $e_2 = 4.78 \times 10^{-3}$, $e_3 = 6.53 \times 10^{-3}$.

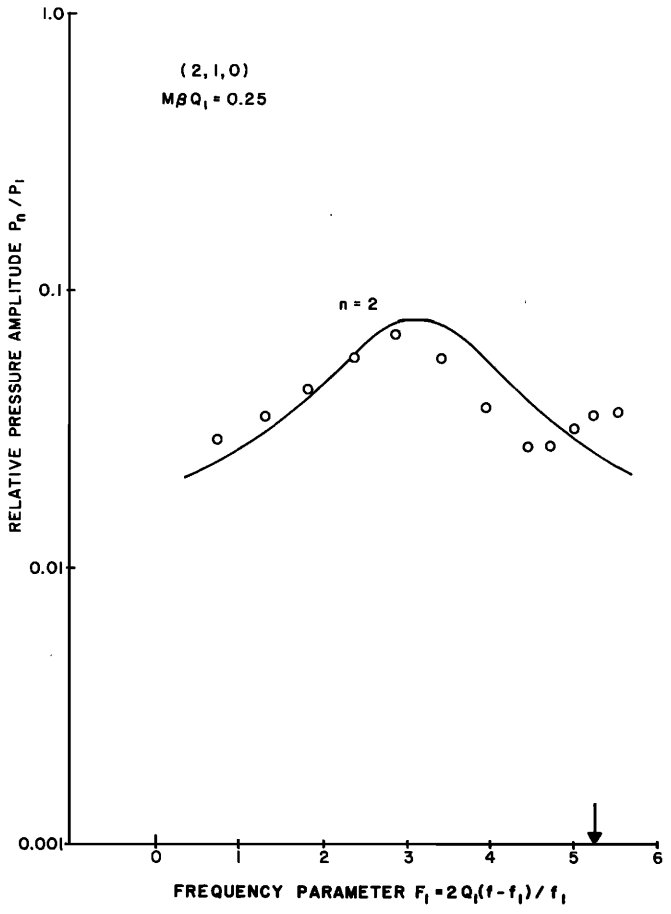

FIG. 8. Finite-amplitude distortion for excitation of the (2, 1, 0) standing wave at a strength parameter of 0.25. Cavity parameters: $Q_1 = 404$, $Q_2 = 500$; $e_2 = 3.79 \times 10^{-3}$.

will follow a line of reasoning based on successive perturbation solutions. Let us designate the individual standing waves that will appear by the notation $(n_x m_x, n_y m_y, n_z m_z; n)$ based on the form of Eqs. 6 and 7.

If the cavity is driven near the resonance frequency of the $(m_x, m_y, m_z; n)$ standing wave, then the first-order, or classical, solution will consist of that standing wave, designated by p_1.

If we solve for the second-order solution p_2 the resulting differential equation is

$$\left(c_2 \Box^2 - \frac{n\omega}{Q_2}\frac{\partial}{\partial t}\right)\frac{p_2}{\rho_0 c_0^2} \doteq -\frac{\partial^2}{\partial t^2}\left[\left(\frac{u_1}{c_0}\right)^2 + \frac{\gamma - 1}{2}\left(\frac{p_1}{\rho_0 c_0^2}\right)^2\right].$$

When all products of the trig functions on the right-hand side are reduced by the identities

$$\sin^2\theta = \tfrac{1}{2}(1 - \cos 2\theta),$$

$$\cos^2\theta = \tfrac{1}{2}(1 + \cos 2\theta),$$

it can be seen that the forcing function is composed of standing waves of the forms $(2m_x, 2m_y, 2m_z; 2n)$ and all permutations of the integers 0 and 2 multiplying the n and m's which we designate by $P(0, 2)$ [for example, $(0, 2m_y, 0; 2n)$, $(2m_x, 0, 0; 0)$, and so forth]. Since the cavity is being driven near the resonance of the p_1 standing wave, for which we have

$$(n\omega/c_0)^2 \approx (n_x m_x \pi/L_x)^2 + (n_y m_y \pi/L_y)^2 + (n_z m_z/L_z)^2,$$

it is then clear that the $(2m_x, 2m_y, 2m_z; 2n)$ is also nearly resonant, and therefore can force a large response. Thus, p_2 will be composed of a very large term $(2m_x, 2m_y, 2m_z; 2n)$ and, barring degeneracies, very small contributions from the other terms in the forcing function. Indeed, study of section I. B. 1 will reveal that all the $P(0, 2)$ terms will yield contributions to p_1 of order $1/Q_2$ with respect to the $(2m_x, 2m_y, 2m_z; 2n)$ term. We therefore retain just this term in the second-order perturbation solution.

The third-order perturbation solution p_3 can be seen to be a solution for the forcing function composed of products of the first- and second-order solutions. Use of the trig reduction formulas for products of sines and cosines of different argument reveals that the products of the standing waves $(m_x, m_y, m_z; n)$ and $2m_x, 2m_y, 2m_z; 2n)$ gives forcing functions composed of the standing waves $(3m_x, 3m_y, 3m_z; 3n)$, $(m_x, m_y, m_z; n)$, and all permutations of the integers 1 and 3 multiplying the n and m's, $P(1, 3)$. Again, barring degeneracies, it can be seen that only the $(3m_x, 3m_y, 3m_z; 3n)$ and $(m_x, m_y, m_z; n)$ lead to nearly resonant responses. (The first of these two terms is the excitation of the third member of the family. The second arises in a perturbation solution as a correction to the first member to account for the energy lost from the p_1 solution in generating the p_2 solution.) Thus, we can approximate p_3 by retaining just the $(3m_x, 3m_y, 3m_z; 3n)$ term. If there is concern about the importance of the interaction of p_1 with the $P(0, 2)$ terms, a little manipulation will reveal that the interaction of $(m_x, m_y, m_z; n)$ with $P(0, 2)$ yields terms $P(1, 3)$ which are of order $1/Q$ with respect to the other $P(1, 3)$ terms arising from the interaction of the $(m_x, m_y, m_z; n)$ and $(2m_x, 2m_y, 2m_z; 2n)$ terms.

Continued application of this process leads to the result that the greatest term in each of the successive perturbation solutions is that of the appropriate family member. This yields the solution given by Eq. 19.

*A few of the results reported herein were presented in preliminary, truncated form at the 1973 Symposium on Finite-Amplitude Wave Effects in Fluids, Technical University of Denmark.

[1]Alan B. Coppens and James V. Sanders, J. Acoust. Soc. Am. 43, 516–529 (1968).

[2]A. B. Coppens, J. V. Sanders, and J. Winn, J. Acoust. Soc. Am. 51, 154(A) (1972).

[3]D. E. Weston, Proc. Phys. Soc. Lond. B66, 695–709 (1953).

[4]Alan B. Coppens and Christopher Lane, J. Acoust. Soc. Am. 54, 336(A) (1973).

[5]D. T. Blackstock, J. Acoust. Soc. Am. 39, 411–413(L) (1966).

[6]R. R. DeVall, "Finite-Amplitude Waves in Imperfect Cavities," M. S. thesis, Naval Postgraduate School (1973).